JACS
JOURNAL OF THE AMERICAN CHEMICAL SOCIETY
Article
pubs.acs.org/JACS

Programmable and Multiparameter DNA-Based Logic Platform For Cancer Recognition and Targeted Therapy

Mingxu You,[†,‡] Guizhi Zhu,[†,‡] Tao Chen,[†,‡] Michael J. Donovan,[†] and Weihong Tan*[,†,‡]

[†]Molecular Science and Biomedicine Laboratory, State Key Laboratory of Chemo/Bio-Sensing and Chemometrics, College of Chemistry and Chemical Engineering, College of Biology, Collaborative Innovation Center for Molecular Engineering and Theranostics, Hunan University, Changsha, Hunan 410082, China

[‡]Department of Chemistry and Physiology and Functional Genomics, Center for Research at the Bio/Nano Interface, Shands Cancer Center, UF Genetics Institute, University of Florida, Gainesville, Florida 32611-7200, United States

Supporting Information

ABSTRACT: The specific inventory of molecules on diseased cell surfaces (e.g., cancer cells) provides clinicians an opportunity for accurate diagnosis and intervention. With the discovery of panels of cancer markers, carrying out analyses of multiple cell-surface markers is conceivable. As a trial to accomplish this, we have recently designed a DNA-based device that is capable of performing autonomous logic-based analysis of two or three cancer cell-surface markers. Combining the specific target-recognition properties of DNA aptamers with toehold-mediated strand displacement reactions, multicellular marker-based cancer analysis can be realized based on modular AND, OR, and NOT Boolean logic gates. Specifically, we report here a general approach for assembling these modular logic gates to execute programmable and higher-order profiling of multiple coexisting cell-surface markers, including several found on cancer cells, with the capacity to report a diagnostic signal and/or deliver targeted photodynamic therapy. The success of this strategy demonstrates the potential of DNA nanotechnology in facilitating targeted disease diagnosis and effective therapy.

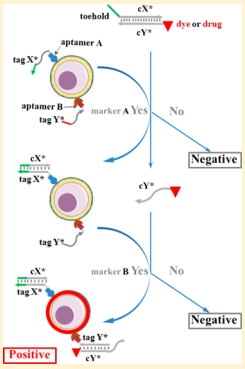

INTRODUCTION

The cell membrane surface consists of thousands of compounds, such as lipids, proteins, and carbohydrates, which play significant roles in cell growth, proliferation, and signaling.[1−4] Particularly, cell-surface receptors, mostly membrane proteins, participate in communication between the cell and the outside world. For example, extracellular signaling molecules, such as cytokines or growth factors, recognize and bind to their receptors, triggering changes in the cell's functions. However, alterations in the expression level and/or function of cell membrane receptors can lead to systemic dysfunction (e.g., aberrant cellular metabolism and proliferation),[5,6] as occurs in cancer cells. Accordingly, more precise identification of the nature of single cells could be achieved by profiling the high or low expression levels of multiple membrane receptors, thus enabling more accurate disease diagnosis and therapy. To accomplish this, we suggest using a molecular assembly of multiple DNA aptamers to build a logic device able to autonomously and precisely target cancer cells, which are otherwise indistinguishable by most single receptor-targeting approaches.

Several interesting combinatorial approaches have been demonstrated to recognize two cell receptors, including the utilization of a proximity-based ligation probe,[7] bispecific antibodies,[8] chimeric costimulatory antigen receptors,[9] and a logic-gated DNA origami robot.[10] These AND-logic gate-based bireceptor-targeting methods have shown some advanced cell discrimination properties, especially in reducing off-target toxicities. However, a more reliable method is required to study complex cellular configurations in large populations of similar cells in biological systems. More recently, we[11] and Rudchenko et al.[12] have independently reported two DNA-based logic systems, which can distinguish diseased cells by examining two or three different expressions of cell surface markers. Compared to the cluster of differentiation (CD) antibodies-based always-ON probe proposed by Rudchenko et al.,[12] we have designed a blueprint that uniquely takes advantage of the nucleic acid nature of the aptamer molecules. The spontaneous activating ability of the structure-switchable aptamers potentially provides a real "autonomous" operation such that the whole process of input-binding/logic-analysis/output-generation can be realized within a single operation.[11] However, none of these previous demonstrations was capable of identifying more complicated cell marker profiles than two-input or AND-gated three-input conditions.

In this report, we develop a general platform to facilitate high-order multiple cell-surface markers identification. This system can assess truth values (0 and 1) based on operations typically taken to be conjunction (AND), disjunction (OR), and negation (NOT), which are the most fundamental logic gates in electronics. Based on DNA cascade reaction platform, we have then implemented a series of aptamer-driven Boolean logical operations into a programmable system. DNA, the chief building block of our logic system, has been widely used to construct devices to perform such intelligent tasks as

Received: September 12, 2014
Published: October 31, 2014

   dx.doi.org/10.1021/ja509263k | J. Am. Chem. Soc. 2015, 137, 667−674

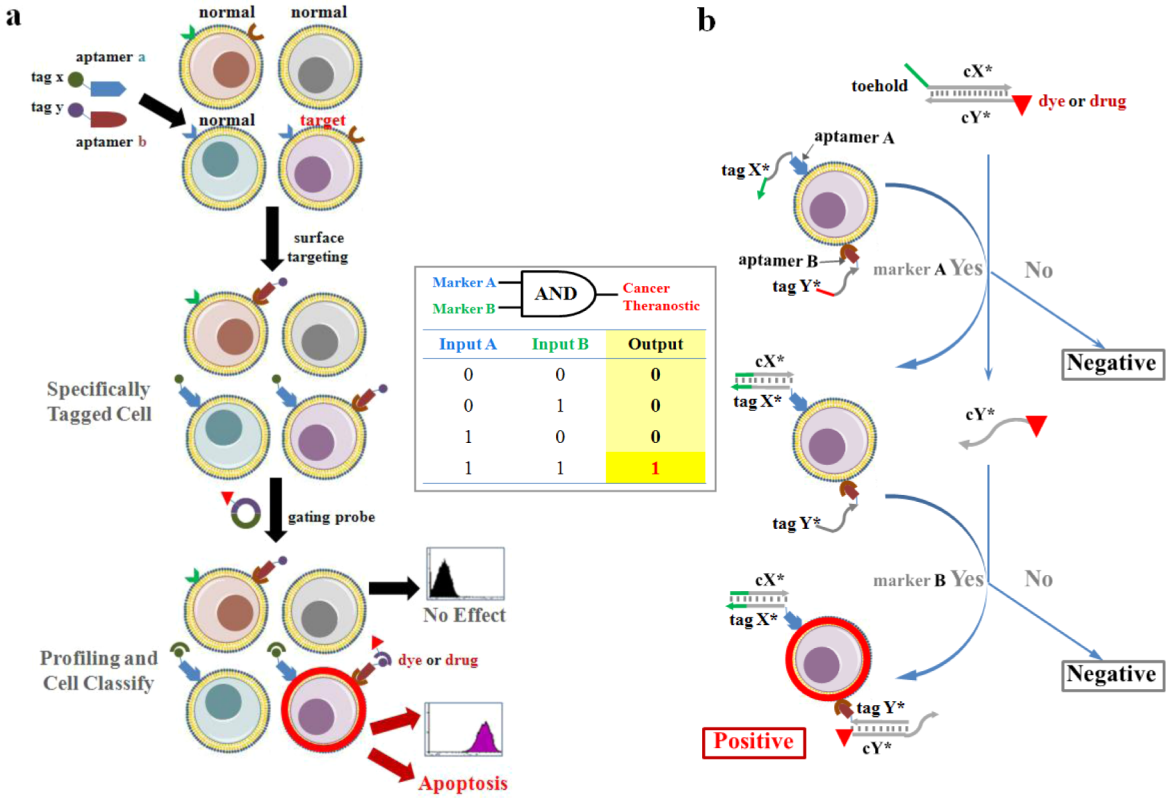

Figure 1. Schemes of the cell-surface logic gates. (A) General principle displayed using two-input "AND" gate as an example. Target cell expressing both membrane receptors (blue and red) can be selected for labeling or apoptosis (red circled cell). Tagged aptamer probes are first incubated with cells, after washing and discarding the nonbinding probes, dye or drug-labeled reporter probe or duplex is added, and the final cellular fluorescence signal or cellular viability is detected with a FACScan cytometer or PI staining assay. (B) Symbols, truth tables, and experimental schemes of toehold-based strand displacement "AND" gate.

sensing[13,14] and computation.[10,15−21] Because of its predictable Watson−Crick hybridization and immense information-encoding capacity, DNA, as a computational tool, can exercise the same capabilities in biomedical applications, considering its ability to combine programmable logic function, nanometer size, and interaction with the biological microenvironment.

The aptamer molecule is a DNA/RNA strand, which is able to selectively recognize a wide range of targets, from small organic/inorganic molecules to proteins.[22−25] Recently, a panel of aptamers has been selected for cell membrane proteins using a process called cell-SELEX.[26] These aptamers demonstrated the ability to identify different expression patterns of the membrane receptors in a variety of cell types.[22] They may even hold the ability to differentiate the same population of cancer cells at various stages of the cell cycle.[26] Our goal here, however, is to use aptamers as an integral component for a molecularly assembled logic device that is able to recognize the expression levels of multiple cell membrane markers. Such a device could (1) deftly survey the biological tapestry of the cancer cell surface, and (2) once having pinpointed the offending cell type, use its feedback mechanism to selectively deliver the appropriate therapeutic reagents. To the best of our knowledge, the realization of such high-order and programmable multi- cellular marker recognition (including 12 three-input conditions and 2 four-input conditions) has never been reported before. The success of this platform will potentially advance our ability in accurate disease diagnosis and effective therapy.

RESULTS

Operational Mechanism. The logic device is based on Boolean operations as shown in Figure 1 and consists of two types of components.[19] The first is a short oligonucleotide tag connected to a specific aptamer probe. Different aptamers may have the same or different tags, and these tags act as barcodes that reflect the cell profiling results. The second component serves as a barcode reader and actuator, with either fluorophore- or therapeutic reagent-labeled ssDNA or dsDNA, whose sequences are designed based on the barcode tags just described. As a result, the actuator can screen the presence or absence of different biological markers on the cell surface and take action after appropriately discriminating the expression patterns of these markers. These two components are not physically linked with each other; instead, they are operationally connected. That is, while the aptamers functionally bind to their cognate cell membrane targets, the tags and actuators functionally execute the logic operations (conjunction, disjunction, negation) based on such recognition.

Boolean Logic Function. In the simplest example, the same tag (named as Y) was introduced to the 3′-end of three well-characterized cancer-targeting aptamer sequences (see Table S1 for all DNA sequences): Sgc8c, against tyrosine-protein kinase-like 7 (PTK7), expressed by cancer cell lines, including human acute lymphoblastic leukemia (CCRF-CEM);[26] TD05, against immunoglobulin heavy μ chain (IgM), expressed by cancer cell lines, including human Burkitt's lymphoma (Ramos);[27] and Sgc4f, whose target protein is not known at this time, targeting both CEM and Ramos cell lines.[26]

dx.doi.org/10.1021/ja509263k | J. Am. Chem. Soc. 2015, 137, 667−674

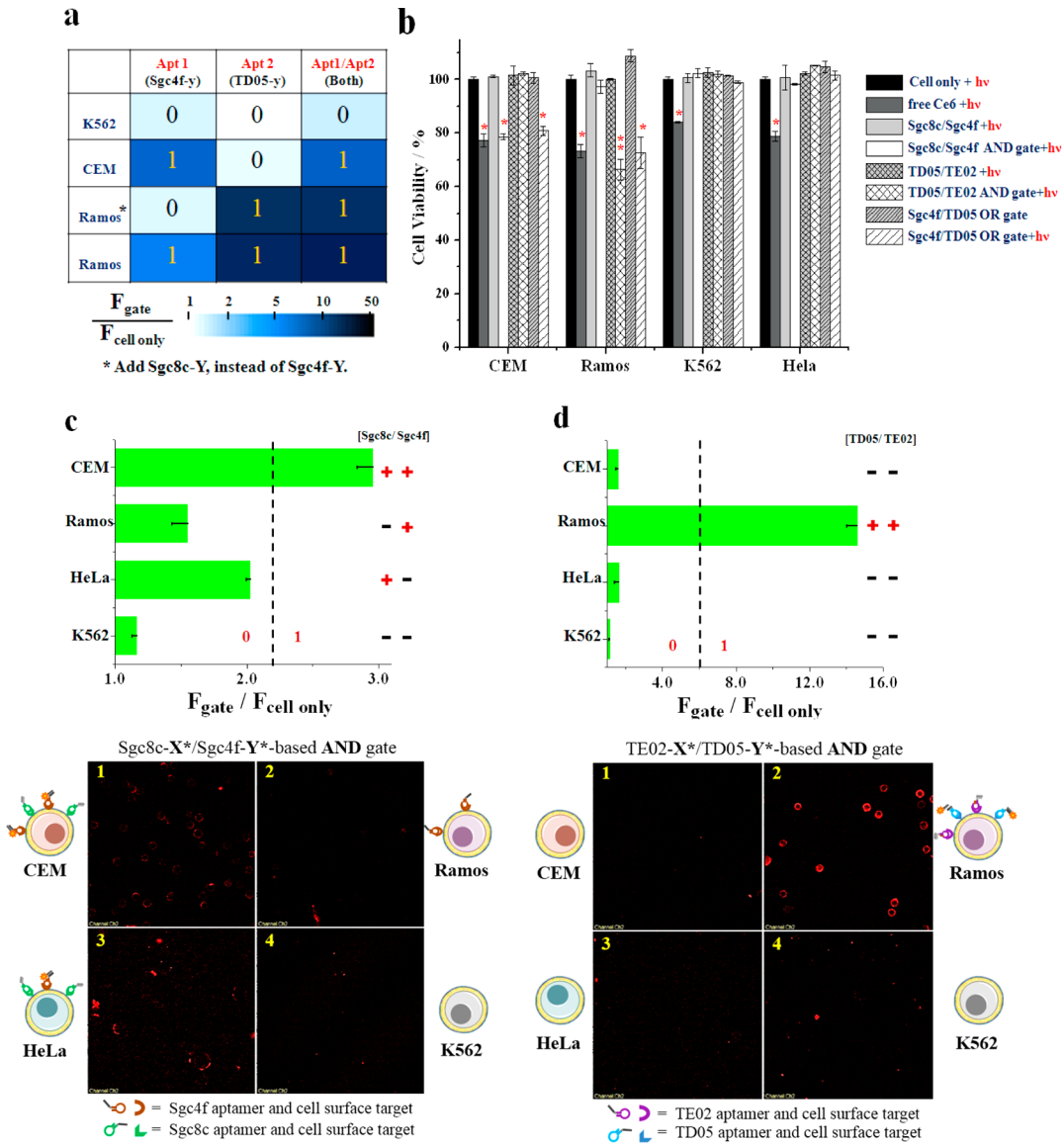

Figure 2. Flow cytometric analysis and comparison of the fluorescence signal with/without the gate probes. (A) "OR" gate, (C) Sgc8c-X*/Sgc4f-Y*-based "AND" gate, and (D) TE02-X*/TD05-Y*-based "AND" gate. The fluorescence values and their error bars (mean ± SD) were calculated based on the FITC signal using channel #3 in the flow cytometer, from three experiments. The relatively high fluorescence signal from the HeLa cells in (C) (Sgc8c+; Sgc4f−) is attributed to the low, but nonzero, expression level of the Sgc4f target (Figure S4). The microscopy images were taken after adding the gate probes to each type of cell, and the expected cell-surface fluorescence patterns were observed; the optical images are shown in the SI. Cell viability test for the (B) "AND" and "OR" gates after visible irradiation for 3 h and subsequent growth for 48 h (*: *p*-value <0.05; **: *p*-value <0.001; by comparison with each irradiated cell type only, $n = 3$).

After aptamer binding to the cell surface, further addition of a fluorescein dye (FAM)-labeled reporter sequence, cY, which is complementary to the Y tag, signals the presence of cells with at least one of the associated markers present. This demonstrates the operation of the OR logic gate with signal ON if any one of the three Y-tagged aptamers exists on the cell membrane (Figure 2A).

In practice, it would be helpful to simultaneously identify the presence of two or more markers on the same cell surface, the equivalent of an AND logic gate [input (1, 1), output 1]. Benefiting from dynamic DNA nanotechnology, the AND gate is designed on the basis of DNA strand displacement reactions, in which two DNA strands hybridize to each other, displacing one or more prehybridized strands through a branch migration.[19,28] A cascade effect results when many such reactions are linked logically. Under these circumstances, a newly released output sequence of one reaction can initiate another strand displacement elsewhere.[28,29]

For our AND gate configuration, a cX*/cY* reporting DNA duplex is partially complementary with a leftover toehold region, and one strand (cY*) is displaced via the toehold by an invading strand (X*), which is the initiator strand for cX* (Figures 1B and S2). The displaced cY* then subsequently hybridizes with invading strand Y* to form yet another new duplex, Y*/cY*, and this represents the second required true input. In our cell-surface AND logic gate, the two invading strands (X* and Y*) are individually tagged onto two types of cancer cell-targeting aptamers (e.g., Sgc8c and Sgc4f), respectively. The rate of strand exchange can be quantitatively controlled[29] by varying the length of the toehold in the

dx.doi.org/10.1021/ja509263k | J. Am. Chem. Soc. 2015, 137, 667−674

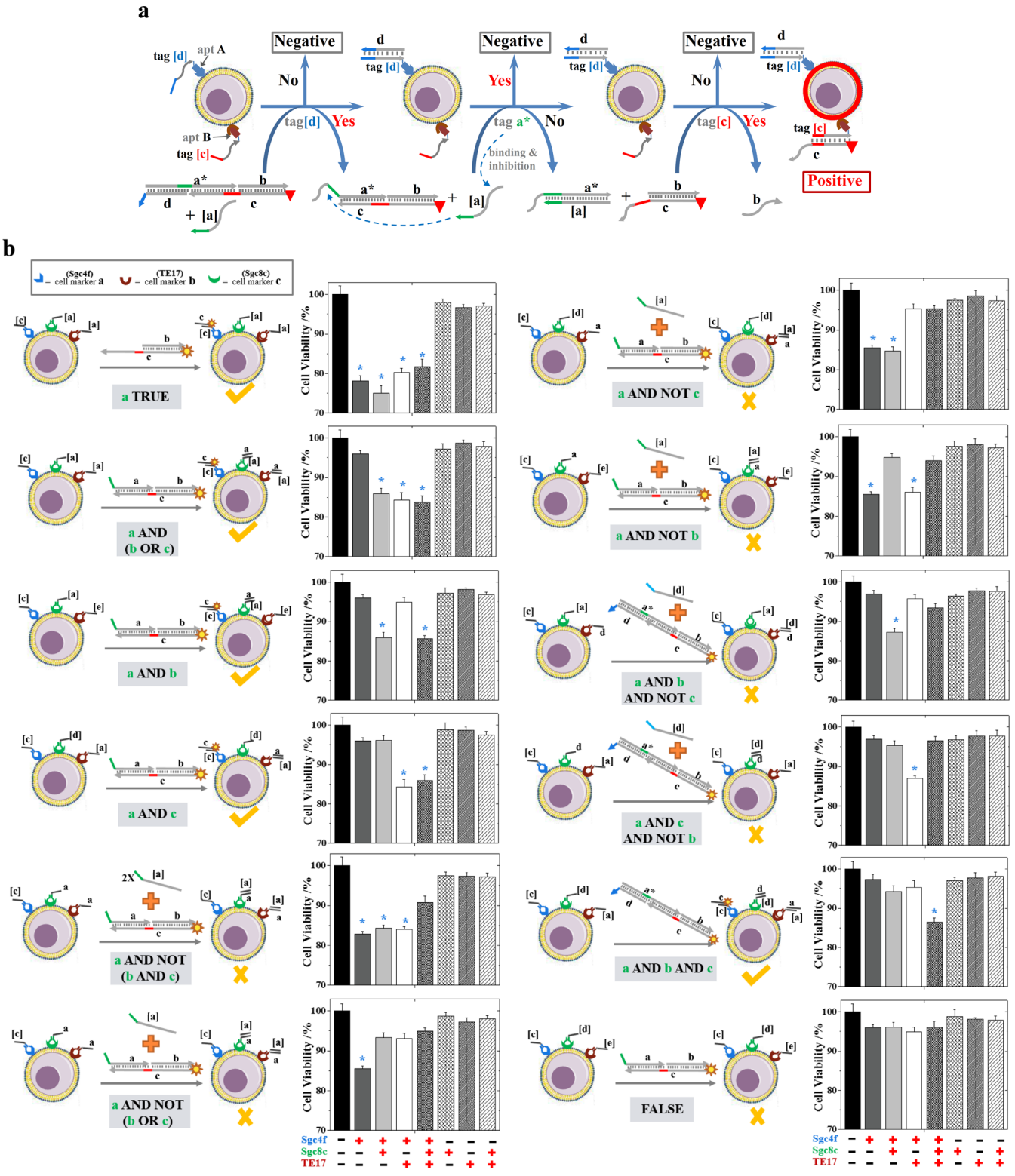

Figure 3. Construction of three-input cell-surface logic gates. (A) Symbols, truth tables, and experimental schemes of three-input "a AND b NOT c" gate. (B) The realization of several three-input cell-surface logic gates, using rationally designed tagged-Sgc4f/Sgc8c/TE17 aptamer pairs and CEM cells as examples (the experimental schemes for each gate are shown in the SI). Cell viability test was performed after visible irradiation for 3 h and subsequent growth for 48 h (*: p-value <0.05; **: p-value <0.001; by comparison with each irradiated cell type only, n = 3). Bracketed letter-labeled strand (e.g., [c] strand) is complementary to the strand labeled with the same letter (e.g., c strand).

reporting duplex (cX*/cY*). Similar to the OR logic gate, the AND gate was tested by adding a fluorescence label to the 3′-end of the reporting duplex (cX*/cY*-FAM). The targeted labeling was achieved only when both barcode tags were attached to the cell surface, i.e., when both inputs were true (Figure S3). More specifically, ON signaling (output 1) is possible only if both sets of aptamer-targeting antigens are present on the cell surface (e.g., CCRF-CEM cells); conversely,

dx.doi.org/10.1021/ja509263k | J. Am. Chem. Soc. 2015, 137, 667−674

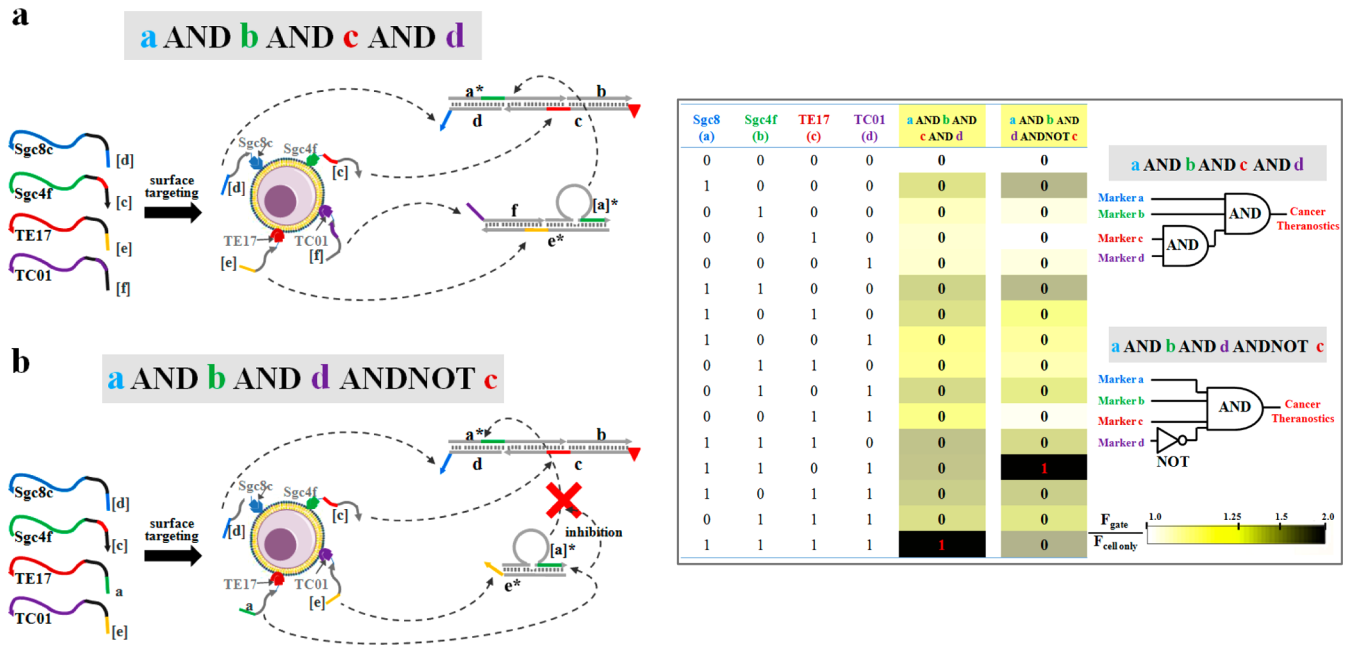

Figure 4. Construction of programmable and scalable cell-surface logic machines. The realization of (A) four-input "a AND b AND c AND d" gate, and (B) four-input "a AND b AND d NOT c" gate. The fluorescence intensity results in the truth table were based on averaged flow cytometry distributions, from three experiments. Bracketed letter-labeled strand (e.g., [d] strand) is complementary to the strand labeled with the same letter (e.g., d strand).

OFF signaling (output 0) is observed in the absence of either one of the receptors (e.g., either Ramos cells or epitheloid cervix carcinoma cells, HeLa) or both receptors (e.g., human erythromyeloblastoid leukemia cells, K562, Figure 2C). This DNA strand displacement design can be generalized for different aptamer-based mapping systems. For example, based on the same pair of oligonucleotide tags, we have achieved another AND gate operation targeting Ramos cells, from the binding of another set of tagged aptamers, TD05-Y* and TE02-X*[27] (Figure 2D).

Targeted Therapy. In addition to analyzing the expression levels of cell-surface receptors, such as those targeted by Sgc8c and Sgc4f, these DNA-based logic devices can trigger a response to produce a targeted therapeutic effect by activating a biologically effective molecule, instead of an output fluorescence signal. For example, a porphyrin-based photosensitizer, chlorine e6 (Ce6), was employed to induce the generation of reactive oxygen species (ROS) upon light irradiation, termed photodynamic therapy (PDT).[30,31] Because of the limited therapeutic window, which equals the traveling distance of ROS, specific localization of the photosensitizer at the diseased site is required for efficient PDT. The triggering response has been tested previously by incorporating Ce6 with the reporter probes,[11] and cell viability was determined by propidium iodide (PI) staining after incubation with the aptamer-based logic gate complex and Ce6-receptor probe. As shown in Figure 2B, efficient specific photoinduced therapy was achieved for target cancer cells expressing abnormal levels of surface markers.

Multilayer Logic Operations. Based on two-input AND, OR, and NOT logic gates, a complex logic system can be sequentially built, including, e.g., the identification of three input membrane markers targeted by Sgc4f, Sgc8c and TE17 aptamers, respectively. As mentioned above, the cascade effect can be realized when many DNA strand displacements are linked such that the newly released output sequence of one reaction can initiate another strand displacement elsewhere.

In a practical application of such higher-order logic operation, after a group of specific oligonucleotide tag-connected aptamers bound with cell membrane markers, three types of actuator strands will be added to realize the identification and targeted therapy. The first is a reporter strand, the fluorophore- or therapeutic reagent-labeled oligonucleotide that provides the fluorescence readout for detection or therapeutic functions after binding with the specific tags on the cellular membrane. The second is one or more gate strands, which is prehybridized with the reporter strand with a leftover toehold region. Several gate strands can function in cascade when they are designed to be partially complementary with each other (Figure 3A). The gate strands function by hybridizing with membrane tags of the complementary sequence and through strand displacement reactions, free the reporter strand for final signaling. The third is an assistant strand, whose sequence is complementary to one of the gate strands and can displace/free the reporter strand. However, the presence of a cell membrane tag with the same sequence as the gate strand will inhibit the activation process, since the assistant strand will preferentially bind to fully complementary (36 bp) free tag, instead of the short toehold region (8 bp) of the gate strand.[28] The assistant strand functions for the realization of a NOT gate, i.e., the presence of a cell membrane input inhibits the activation of the fluorescence signal or therapeutic effect. These three types of strands are rationally designed in our platform to function together as the barcode reader and actuator.

To illustrate this whole process, the operation of an AND/AND-NOT gate system was assembled from a reporter strand (c), an assistant strand ([a]) and three gate strands (a*, b, and d) (Figure 3A). As shown in Figure 3, Sgc4f, Sgc8c, and TE17 aptamers, which were individually tagged by strands [c], a*, or [d], were used to introduce specific barcode tags onto the CEM

dx.doi.org/10.1021/ja509263k | J. Am. Chem. Soc. 2015, 137, 667−674

cell membrane and to realize the "Sgc4f AND Sgc8c AND-NOT TE17" and the "Sgc4f AND TE17 AND-NOT Sgc8c" gates. To understand how the barcode reader strands work in practice, once the first input on the cell membrane removes the first gate strand (d) and exposes the second toehold, the assistant strand ([a]) will automatically displace the second gate strand (a*), an event which facilitates binding of the second input strand ([c]) with the reporter strand (c) and transmits signals.

The assistant probes, e.g., [a] strand in this example, will preferentially bind to fully complementary free a* tag in the cell-surface aptamer strand, instead of the reporting DNA nanostructure (a*/b/c-biotin), which involves a competition effect from b and c strands. As a result, a NOT gate is realized, since the presence of a cell membrane input (targeted by a*-tagged aptamer) inhibits the binding of [a] strand with the toehold region of the a* gate strand. The concentration of the assistant probe is dependent on the amount of the safeguard receptors on the cell membrane (more on normal cells, but much less on cancer cells, which are targeted by a NOT gate aptamer) (Figure 3A). The optimization of these assistant probe concentrations can be used to fine-tune the logic-based therapeutic effect and, subsequently, even to realize different logic operations. For example, the ability to distinguish between the "Sgc4f AND-NOT (TE17 AND Sgc8c)" and "Sgc4f AND-NOT (TE17 OR Sgc8c)" gates can be realized by altering the concentration of assistant probe [a] (Figures 3 and S8).

NOR [output is 1 only if both inputs are false (0, 0)] and NAND [output is 0 only if both inputs are true (1, 1)] gates are unique, since they are functionally complete, i.e., any computational logic system could be built by scaling up either one of these two gates. The realization of AND and NOT gates provides the basis for building up these two types of important logic gates, as demonstrated in schemes (e) and (f) in Figure S7. More specifically, the logic platform demonstrated here can realize all the possible 256 kinds of logic gates for three-input cell surface logic systems; more practically, since at least one aptamer is required to bind on the cell membrane to transmit the signal, 128 kinds can be achieved. As a result, the cell surface condition of "receptor a^-/ receptor b^-/ receptor c^-" will always be reported as 0.

To demonstrate the modularity and scalability of DNA-based approaches that are similarly based on the rational tagging of specific barcode tags to the cell-targeting aptamers, we proved the successful operation of another 10 three-input logic gates (Figure 3) and 2 four-input systems, "Sgc8c AND Sgc4f AND TE17 AND TC01" and "Sgc8c AND Sgc4f AND TC01 AND-NOT TE17" (Figure 4). The detailed experimental schemes for individual gates are displayed in Figure S7, in which both a targeted therapeutic effect and a cell surface fluorescence signal from flow cytometry proved the proper function of the logic device.

DISCUSSION

Even though most tested high-order logic operations function as expected, as the layer of the gates scale up, we have observed that the diagnostic signals, as well as the therapeutic effects, subsequently decrease. For example, some positive signals are difficult to be distinguished from the negative ones in both "Sgc4f AND-NOT (TE17 AND Sgc8c)" and "Sgc4f AND TE17 AND-NOT Sgc8c" gates. This effect can be due to the incomplete strand displacement during each step and the relatively slow kinetics of some of these reactions.[28] To solve this problem, our follow-up project involves the incorporation of signal amplification methods, such as the hybridization chain reaction[32,33] or rolling circle amplification,[7] into this logic platform. Moreover, the therapeutic efficiency of the current high-order logic platform is still limited (20−30% decrease in cell viability), which is partially due to the relatively low efficiency of the Ce6-based photodynamic therapy system.[30,31] Due to the facile synthesis and modification of DNA probes, in this logic platform, the Ce6 moiety can be easily replaced with other drugs, reporting systems, or nanoparticles.

For future clinical applications, some artificial nucleotides should be introduced to further enhance the biostability of the nucleic acid−based logic platform in complex biological systems, such as serum. Using the "A AND B" gate as an example, one potential limit of the current system stems from the condition of neighboring cells expressing marker A or B, respectively, which might report a joint "positive" signal to confound the results. To avoid such false-positives, we have recently reported the possible construction of a physically conjugated DNA assembly that is based on toehold-mediated strand displacement reactions, termed the "Nano-Claw".[11] Two examples, including a conjugated two-input AND gate and a three-input AND-AND gate, were realized. The new and highly programmable logic platform demonstrated in the current study can be easily integrated with the Nano-Claw device, to realize more powerful cellular identification and therapeutic applications. However, the goal of the current study has been already fulfilled with the demonstration that a high-order DNA-based logic platform is capable of programmable targeting cancer cells with much more complicated marker profiles.

In conclusion, based on a series of aptamer-encoded AND, OR, and NOT logic gates, we have designed and realized a programmable and general platform that screen for various abnormal conditions on the cell surface. The Boolean operations that support these logic operations can be further programmed to build more complex and highly functional logic systems. Specifically, by coupling multiple molecular signature inputs into a fluorescence signal or therapeutic modality, e.g., PDT, a diagnostic assessment and/or therapeutic action can be taken. This integrated multiligand profiling approach will be a major advancement over single-ligand systems and will prevent extraneous target effects on normal cells. The predictable and programmable nature of the nucleic acid probes can be employed to construct smarter devices for applications in basic research, biomedical engineering, and personalized medicine.

MATERIALS AND METHODS

Chemicals, Cell Lines, and Reagents. The materials for DNA synthesis were purchased from Glen Research (Sterling, VA), including 6-(3′,6′-dipivaloylfluoresceinyl-6-carboxamido)-hexyl-phosphoramidite (6-FAM) and 5′-amino phosphoramidite. Photodynamic ligand chlorine e6 (Ce6) was purchased from Frontier Scientific, Logan, UT. Other chemicals were purchased from Sigma-Aldrich. HeLa cells were cultured in DMEM medium (Sigma), and CCRF-CEM (CCL-119, T-cell line, human ALL), Ramos (CRL-1596, B-cell line, human Burkitt's lymphoma), and K562 (CCL-240, acute promyelocytic leukemia, CML) were cultured in RPMI 1640 medium (American Type Culture Collection) with 10% fetal bovine serum (Invitrogen, Carlsbad, CA) and 0.5 mg/mL penicillin-streptomycin (American Type Culture Collection) at 37 °C under a 5% CO_2 atmosphere. Cells were washed before and after incubation with washing buffer [4.5 g/L glucose and 5 mM $MgCl_2$ in Dulbecco's PBS with calcium chloride and magnesium chloride (Sigma-Aldrich)]. Binding buffer was prepared by adding yeast tRNA (0.1 mg/mL;

Sigma-Aldrich) and BSA (1 mg/mL; Fisher Scientific) to the washing buffer to reduce background binding. All reagents for buffer preparation and HPLC purification came from Fisher Scientific. Unless otherwise stated, all chemicals were used without further purification.

DNA Synthesis. All oligonucleotides were synthesized using an ABI 3400 DNA synthesizer (Applied Biosystems, Inc., Foster City, CA) at the 1.0 μmol scale. After complete cleavage and deprotection, the DNA sequences were purified on a ProStar HPLC system (Varian, Palo Alto, CA) with a C-18 reversed-phase column (Alltech, 5 μm, 250 × 4.6 mm). The eluent was 100 mM triethylamine-acetic acid buffer (TEAA, pH 7.5) and acetonitrile (0−30 min, 10−100%). All DNA concentrations were characterized with a Cary Bio-300UV spectrometer (Varian) using the absorbance of DNA at 260 nm.

Synthesis of Photosensitizer-Modified Oligonucleotides. The 5′-amino-modified oligonucleotide was synthesized, and the MMT protection group removed using an ABI 3400 DNA synthesizer in order to conjugate the carboxyl group with the Ce6 molecule. To improve the coupling efficiency and reduce the number of multiple coupling products, the amount of Ce6 was 10 times that of the oligonucleotides in the coupling reaction. In a typical reaction, 10 μmol Ce6 was mixed with an equivalent amount of coupling agents, *N*,*N*′-dicyclohexylcarbodiimide (DCC) and *N*-hydroxysuccinimide (NHS), in 500 μL *N*,*N*-dimethylformamide (DMF) for the activation reaction. The product was then washed with acetonitrile until clear, dried using a vacuum dryer, and further purified by reversed-phase HPLC.

Manipulation of the Logic Gates. The pre-annealed DNA duplex was prepared by a cooling process from 95 to 4 °C over 30 min in a 12 mM PBS buffer (pH = 7.4 with 137 mM NaCl and 2.7 mM KCl); other DNA probes were cooled on ice for 10 min before usage. Tagged aptamer probes were incubated at a concentration of 200 nM with 10^6 cells per mL in 200 μL binding buffer and shaken on ice for 30 min. After washing and discarding the nonbinding probes, 200 nM FAM-labeled reporter probe or duplex was added for 1 h of strand binding and incubation on ice. After further washing to remove nonbinding probes, the final detection of cellular fluorescence signal was performed with a FACScan cytometer (Becton Dickinson Immunocytometry Systems, San Jose, CA) by counting 20 000 events, using channel #3 for the FAM dye and channel #5 for the PE-Cy5.5 dye.

Photodynamic Therapy and Cell Viability Test. The cell viability of different cell lines was determined using the PI staining assay (Molecular Probes Inc., Eugene, OR). At first, the cells (100 000 cells/well) were incubated with the logic machines, following the above-mentioned method. For photodynamic therapy, the cells were separately placed in a 48-well plate on ice for 3 h irradiation with white light (15 W, 60 Hz table lamp). After irradiation, the cells were incubated in culture medium at 37 °C under 5% CO_2 atmosphere for further cell growth (48 h). To measure the cell viability, 1.5 μL PI (10-fold dilution from 1.0 mg/mL water solution) was added to each well and incubated for 15 min at room temperature before analyzing cells on the flow cytometer. Using channel #4 for the PI dye, 10 000 events were counted for each well.

Formation and Purification of DNA Nanostructures for the Three- and Four-Input Cell-Surface Logic Operations. The pre-annealed DNA nanostructure was prepared by a slower cooling process from 95 °C to room temperature overnight in a 12 mM PBS buffer (pH = 7.4 with 137 mM NaCl and 2.7 mM KCl). Each nanostructure for different gates was separately purified from a gel electrophoresis experiment. The gel was run in 10% acrylamide (containing 19/1 acrylamide/bis(acrylamide)) mixture with 1 × TBE/15 mM Mg^{2+} buffer, at 100 V constant voltage for 1.5 h (4 °C). This gel purification process allowed the removal of partially assembled structures and decreased the number of false-positive signals. After purification, the concentrations of DNA nanostructures were characterized with a Cary Bio-300UV spectrometer (Varian) using the absorbance of DNA at 260 nm. The extinction coefficients for the formed nanostructures were calculated from the equation:[34] $\varepsilon_{ds} = \varepsilon_{ss}(\text{str1}) + \varepsilon_{ss}(\text{str2}) - 3200 \times N_{AT} - 2000 \times N_{GC}$, where ε_{ss}(str1) and ε_{ss}(str2) are the extinction coefficients of each component single strand in the duplex, and N_{AT} and N_{GC} are the number of A-T and G-C pairs in the duplex form, respectively.

Manipulation of the Three- and Four-Input Cell-Surface Logic Operations. The pre-annealed DNA nanostructure was prepared as mentioned above; other DNA probes were cooled on ice for 10 min before usage. Tagged aptamer probes were incubated at a concentration of 200 nM with 10^6 cells per mL in binding buffer on ice and shaken for 30 min. After washing and discarding the nonbinding probes, 200 nM Biotin-labeled DNA nanostructure for each gate was added for 4 h of strand binding and incubation on ice. Then, 50 nM assistant probe (a or d strand) was added for each NOT gate; 100 nM assistant probe (a strand) was added for the "a AND NOT (b AND c)" gate. After further washing to remove nonbinding probes, steptavidin-tagged PE-Cy5.5 dye was added (free PE-Cy5.5 dye was removed after 15 min incubation), and the final detection of cellular fluorescence signal was performed with a FACScan cytometer (Becton Dickinson Immunocytometry Systems, San Jose, CA) by counting 20 000 events, using channel #5.

■ ASSOCIATED CONTENT

Supporting Information

This material is available free of charge via the Internet at http://pubs.acs.org.

■ AUTHOR INFORMATION

Corresponding Author

tan@chem.ufl.edu

Notes

The authors declare no competing financial interest.

■ ACKNOWLEDGMENTS

This work is supported by the National Key Scientific Program of China (2011CB911000), NSFC grants (NSFC 21221003 and NSFC 21327009), and China National Instrumentation Program 2011YQ03012412 and by the National Institutes of Health (GM079359 and CA133086).

■ REFERENCES

(1) Garnett, M. J.; et al. *Nature* **2012**, *483*, 570−575.
(2) Vivier, E.; Ugolini, S.; Blaise, D.; Chabannon, C.; Brossay, L. *Nat. Rev. Immunol* **2012**, *12*, 239−252.
(3) Revankar, C. M.; Cimino, D. F.; Sklar, L. A.; Arterburn, J. B.; Prossnitz, E. R. *Science* **2005**, *307*, 1625−1630.
(4) Mager, M. D.; LaPointe, V.; Stevens, M. M. *Nat. Chem.* **2011**, *3*, 582−589.
(5) Hollingsworth, M. A.; Swanson, B. J. *Nat. Rev. Cancer* **2004**, *4*, 45−60.
(6) Png, K. J.; Halberg, N.; Yoshida, M.; Tavazoie, S. F. *Nature* **2012**, *481*, 190−194.
(7) Söderberg, O.; et al. *Nat. Methods* **2006**, *3*, 995−1000.
(8) Holmes, D. *Nat. Rev. Drug Discovery* **2011**, *10*, 798−800.
(9) Kloss, C. C.; Condomines, M.; Cartellieri, M.; Bachmann, M.; Sadelain, M. *Nat. Biotechnol.* **2013**, *31*, 71−75.
(10) Douglas, S. M.; Bachelet, I.; Church, G. M. *Science* **2012**, *335*, 831−834.
(11) You, M. *J. Am. Chem. Soc.* **2014**, *136*, 1256−1259.
(12) Rudchenko, M. *Nat. Nanotechnol.* **2013**, *8*, 580−586.
(13) Krishnan, Y.; Simmel, F. C. *Angew. Chem., Int. Ed. Engl.* **2011**, *50*, 3124−3156.
(14) Liu, J.; Cao, Z.; Lu, Y. *Chem. Rev.* **2009**, *109*, 1948−1998.
(15) Benenson, Y.; Gil, B.; Ben-Dor, U.; Adar, R.; Shapiro, E. *Nature* **2004**, *429*, 423−429.
(16) Qian, L.; Winfree, E. *Science* **2011**, *332*, 1196−1201.
(17) Xie, Z.; Wroblewska, L.; Prochazka, L.; Weiss, R.; Benenson, Y. *Science* **2011**, *333*, 1307−1311.

(18) Gil, B.; Kahan-Hanum, M.; Skirtenko, N.; Adar, R.; Shapiro, E. *Nano Lett.* **2011**, *11*, 2989−2996.
(19) Seelig, G.; Soloveichik, D.; Zhang, D. Y.; Winfree, E. *Science* **2006**, *314*, 1585−1588.
(20) Pei, R.; Matamoros, E.; Liu, M.; Stefanovic, D.; Stojanovic, M. N. *Nat. Nanotechnol.* **2010**, *5*, 773−777.
(21) Elbaz, J.; et al. *Nat. Nanotechnol.* **2010**, *5*, 417−422.
(22) Fang, X.; Tan, W. *Acc. Chem. Res.* **2010**, *43*, 48−57.
(23) Breaker, R. R. *Nature* **2004**, *432*, 838−845.
(24) Sefah, K.; Shangguan, D.; Xiong, X.; O'Donoghue, M. B.; Tan, W. *Nat. Protoc.* **2010**, *5*, 1169−1185.
(25) Famulok, M.; Hartig, J. S.; Mayer, G. *Chem. Rev.* **2007**, *107*, 3715−3743.
(26) Shangguan, D.; et al. *Proc. Natl. Acad. Sci. U. S. A.* **2006**, *103*, 11838−11843.
(27) Tang, Z.; et al. *Anal. Chem.* **2007**, *79*, 4900−4907.
(28) Zhang, D. Y.; Seelig, G. *Nat. Chem.* **2011**, *3*, 103−113.
(29) Zhang, D. Y.; Winfree, E. *J. Am. Chem. Soc.* **2009**, *131*, 17303−17314.
(30) Castano, A. P.; Mroz, P.; Hamblin, M. R. *Nat. Rev. Cancer* **2006**, *6*, 535−545.
(31) Lovell, J. F.; Liu, T. W.; Chen, J.; Zheng, G. *Chem. Rev.* **2010**, *110*, 2839−2857.
(32) Zhu, G.; et al. *Proc. Natl. Acad. Sci. U. S. A.* **2013**, *110*, 7998−8003.
(33) Han, D.; et al. *ACS Nano* **2013**, *7*, 2312−2319.
(34) Puglisi, J. D.; Tinoco, I. *Methods Enzymol.* **1989**, *180*, 304−325.